Bioorganic Chemistry 88 (2019) 102947

Contents lists available at ScienceDirect

Bioorganic Chemistry

journal homepage: www.elsevier.com/locate/bioorg

Isolation, identification, and quantification of Pentylcurcumene from *Geophila repens*: A new class of cholinesterase inhibitor for Alzheimer's disease

Umesh Chandra Dash[a], Satish Kanhar[a], Anshuman Dixit[b], Jagnehswar Dandapat[c], Atish Kumar Sahoo[a,*]

[a] Medicinal & Aromatic Plant Division, Regional Plant Resource Centre, Forest & Environment Department, Govt. of Odisha, Nayapalli, Bhubaneswar 751015, India
[b] Institute of Life Sciences (ILS), NALCO Square, Bhubaneswar-751023, Odisha, India
[c] Department of Biotechnology, Utkal University, Vani Vihar, Bhubaneswar 751004, India

ARTICLE INFO

Keywords:
Pentylcurcumene
Geophila repens
CAP-e
ORAC
Bioautography
HPTLC
Molecular docking
Acetylcholinesterase
Butyrylcholinesterase
Alzheimer's disease

PubChem CIDs:
Pentylcurcumene (PubChem CID: 91710308)
2,2-diphenyl-1-picrylhydrazyl (PubChem CID: 74358)
Acetylcholinesterase (PubChem SID: 318693250)
Acetylthiocholine iodide (PubChem CID:

ABSTRACT

The aerial part of *Geophila repens* (L.) I.M. Johnst (Rubiaceae) has been used in India to improve intelligence and memory for a long time. As part of our ongoing efforts in discovering potential bioactive compounds from *G. repens*, we have studied the isolation, identification, and quantification of a new class of cholinesterase inhibitor from *G. repens* for Alzheimer's disease (AD). Terpene was isolated from hydroalcohol extract of *G. repens* (GRHA) and its structure was identified "Pentylcurcumene" by spectroscopic data. HPTLC fingerprint analysis was performed and good separation was achieved in mobile phase (benzene:methanol; 7.5:2.5, v/v, 254 and 366 nm; R_f 0.51). The method was validated using ICH guidelines in terms of linearity, specificity, sensitivity, accuracy, precision, robustness and stability. In cellular antioxidant studies e.g. DPPH, oxygen-radical-absorbance-capacity (ORAC) and cell-based-antioxidant-protection-in-erythrocytes (CAP-e) assays showed that, Pentylcurcumene showed remarkably different degrees of antioxidant activities in dose-dependent manner. Pentylcurcumene demonstrated anticholinesterase activities e.g. IC_{50} of acetylcholinesterase (AChE) and butyrylcholinesterase (BChE) inhibition were 73.12 ± 0.56 and 97.65 ± 0.46 μg/ml, respectively. To better understand enzyme kinetics, Lineweaver-Burk plot of Pentylcurcumene displayed the highest affinity with competitive inhibition (reversible) towards both AChE (V_{max} 0.8) and BChE (V_{max} 0.6). An improved and advanced HPTLC tool of bioautography detection of Pentylcurcumene has been successfully demonstrated its anticholinesterase activities. Molecular docking simulations of Pentylcurcumene (ligand) and enzymes (proteins) exhibited the binding of ligand at active sites of AChE (human/rat) and BChE (human/homology) efficiently and also predicted the

Abbreviations: PC, Pentylcurcumene; AChE, acetylcholinesterase; BChE, butyrylcholinesterase; GRHA, hydroalcohol extract of *Geophila repens*; UV, ultra violet; IR, infrared; ^{1}H NMR, proton nuclear magnetic resonance; ^{13}C NMR, carbon-13 nuclear magnetic resonance; HR-MS, high-resolution mass spectrometry; HPTLC, high-performance thin-layer chromatography; IC_{50}, half maximal inhibitory concentration; ORAC, oxygen radical absorbance capacity; CAP-e, cell based antioxidant protection in erythrocytes; SARs, Structure-activity relationships; PDB, protein data bank; AD, Alzheimer's disease; HPLC, high performance liquid chromatography; DPPH, 2,2-diphenyl-1-picrylhydrazyl; SBTC, S-butyrylthiocholine chloride; ATCI, acetylthiocholine iodide; DTNB, 5,5′-dithio-bis-(2-nitrobenzoic acid); AAPH, 2,2′-azobis (2-amidino-propane) dihydrochloride; DCF-DA, 2′,7′-dichlorofluorescin diacetate; TLC, thin layer chromatography; R_f, retardation factor; ICH, International conference on Harmonization; LOD, limit of detection; LOQ, limit of quantification; COSY, correlated spectroscopy; HMBC, heteronuclear multiple-bond correlation spectroscopy; SD, standard deviation; SEM, standard error mean; RSD, relative standard deviation; Ex., excitation; Em., emission; Trp, Tryptophan; Phe, Phenylalanine; Tyr, Tyrosine; Leu, Leucine; Val, Valine

* Corresponding author at: Medicinal & Aromatic Plant Division, Regional Plant Resource Centre, Forest & Environment Department, Govt. of Odisha, Nayapalli, Bhubaneswar 751015, India.
E-mail address: atish_kumar1976@yahoo.co.in (A.K. Sahoo).

https://doi.org/10.1016/j.bioorg.2019.102947
Received 30 January 2019; Received in revised form 25 March 2019; Accepted 20 April 2019
Available online 22 April 2019

74629)
S-butyrylthiocholine chloride (PubChem CID: 3015121)
5,5′-dithio-bis-(2-nitrobenzoic acid) (PubChem CID: 6254)
Fluorescein Sodium Salt (PubChem SID: 24894907)
2,2′-azobis (2-amidino-propane) dihydrochloride (PubChem CID: 84924)
2′,7′-dichlorofluorescin diacetate (PubChem CID: 77718)

hydrophobic interaction of drug towards different amino acid residue within proteins. As per the results of antioxidant study and with the support of molecular docking analysis, it is concluded that Pentylcurcumene could be a potential first-line cholinesterase-inhibitor for AD.

1. Introduction

Alzheimer's disease (AD) is one of the most recognised neurodegenerative diseases that impairs memory, cognitive functions and may lead to dementia in late stage of life. The cause of neuronal cell dysfunction leading to the memory loss in AD is poorly understood due to the complex pathologic features e.g. cholinergic deficiency, Aβ-plaques and hyperphosphorylated τ-protein, reactive oxygen species (ROS), mitochondrial dysfunction etc. Acetylcholine is the neurotransmitter, responsible for cholinergic dysfunction and cognitive deficits, which leads amyloid plaques in AD patients and causes amyloid toxicity in brain. The U.S. Food and Drug Administration (FDA) approved most of the synthetic or natural drugs are partial inhibitors rather than curative such as tacrine, donepezil, rivastigmine, and galantamine, Huperzine A, gingkolides [1]. All these first-line cholinesterase-inhibitors have been widely used for the symptomatic treatments in AD, whereas it has failed in several aspects because of complex pathologic features. Therefore, new drugs that block the disease-inducing mechanisms are essential [1,2].

Geophila repens (L.) I.M. Johnst (Rubiaceae) is commonly known as "Snake Pennywort", in Sanskrit it is known as "Krishnamanduki" and, locally called as "Karimuthil". It is a small creeping perennial herb, commonly found in India, China, and other Southeast Asian countries. In traditional systems of medicine, the plant is used to cure many diseases, as the aerial parts are used in cough, diarrhoea, oedema, leprosy, piles, fever, inflammatory swellings, antimicrobial, antifungal, and memory enhancing properties [3]. However, there is no scientific proof behind these traditional medicines. Proving the traditional claim scientifically; antioxidant, and anticholinesterase activities of *G. repens* were initially studied by authors. Experimental evidences of our earlier work on HPTLC bioautographic test shows the localization of bioactivity molecules within the plant extract were responsible for anticholinesterase activities [3]. As part of our ongoing efforts in discovering potential bioactive compounds from *G. repens*; advances in extraction and isolation techniques have been followed to develop cholinesterase inhibitors from *G. repens*. Among many natural products, terpenes are the largest and the most diverse group of natural compounds, which have been identified as potential drugs for AD e.g. (+)- and (−)-α-pinenes, (+)-3-carene and S-(+)-linalool are the AChE inhibitors and restore the cognitive functions in AD [4,5].

The study highlights the isolation, structural elucidation and quantification of Pentylcurcumene (PC), a terpene from hydroalcohol extract of *G. repens* (GRHA). Extensive literature survey revealed that there are no official analytical methods available for estimation of PC. High performance thin layer chromatography (HPTLC) method has been developed and validated for quantitative determination of PC in *G. repens* because of its reliability in quantitation of analytes at nanogram level, cost effectiveness, simple, and sensitive. Regarding the bioactivity of PC, cellular antioxidant studies e.g. DPPH radical scavenging activities, oxygen radical absorbance capacity (ORAC) and cell-based antioxidant protection in erythrocytes (CAP-e) studies were performed. The advantage of the ORAC assay is the wide range of applications as it can be used for both lipophilic and hydrophilic samples to quantify the antioxidant capacity toward different oxidants e.g. hydroxyl radicals, peroxyl radicals and peroxynitrite [6]. Clinical trial is time consuming and expensive, so *ex vivo* CAP-e was performed to evaluate the antioxidant capacity of PC to protect cells from oxidative damage. In the present study, we investigated the anticholinesterase activities of PC and this observation was further extended to the bioautography detection of PC towards acetylcholinesterase (AChE) and butyrylcholinesterase (BChE) inhibition activities. In addition, enzyme kinetics and computational molecular docking analysis were carried out between receptor (protein) and ligand (PC) to find out inhibitory potential of AChE and BChE in human and mouse homology models in AD.

2. Material and methods

2.1. Reagents and chemicals

Chemicals and solvents were used of analytical and HPLC grade. Acetylcholinesterase (AChE; 1001940206), Butyrylcholinesterase (BChE; 1001390738), S-butyrylthiocholine chloride (SBTC; 1001315809), Acetylthiocholine iodide (ATCI; 101291297), 5,5′-dithio-bis-(2-nitrobenzoic acid) (DTNB; D8130), 2,2′-azobis (2-methylpropionamidine dihydrochloride) (AAPH; 440914), Fluorescein sodium salt (F6377), 2′,7′-dichlorofluorescin diacetate (D6883) and Galanthamine hydrobromide (101454428) were purchased from Sigma-Aldrich, USA. Ultrapure water (Millipore, India) was used in all experiments.

2.2. Plant material collection

The aerial parts of leaves of *Geophila repens* (L.) I.M. Johnst (Rubiaceae), were collected from Barbara forest (19° 52′ 53.9″ N, 85° 03′ 26.2″ E), Khurda district, Odisha, India and was identified by Dr. P. C. Panda, Taxonomist, Regional Plant Resource Centre, Bhubaneswar, India. The voucher specimen was deposited at our centre for future references (7557/RPRC).

2.3. Extraction and isolation

The leaves of *G. repens* were shade dried (25–30 °C) and ground to powder form. The powdered material (2 kg) was extracted with the mixture of alcohol and water in the ratio of 3:7 for 72 h by maceration at room temp. The collected solvent was evaporated under reduced pressure by a rotary evaporator (R-100, Buchi, Switzerland) to get the crude extract (GRHA, 8% w/w) and stored in a desiccator for further experimental work. GRHA (150 g) was subjected to column (Borosil, 100 × 5 cm) chromatography separation for isolation of bioactive principles. GRHA was absorbed by silica gel (100–200 mesh, 400 g) and kept overnight for drying and then packed in column. Column was eluted successively with hexane (100%) to collect 30 fractions (Frs. 1–30; 5 mL each), hexane-chloroform (95:5–0:100, v/v) to collect 260 fractions (Frs. 31–290; 5 mL each). Fraction no. 100–220 (hexane-chloroform, 60:40, v/v) were pooled into a single fraction on the basis

of similar TLC fingerprint pattern (hexane:chloroform:ethylacetate; 6:3:1, v/v) and allowed to dry to obtain a yellow semi solid mass (2.4 g). It was then further subjected to column (Borosil, 75 × 2.54 cm) chromatography separation of mixtures using hexane (100%), hexane:chloroform (95:05, 90:10; 85:15; 80:20; 75:25; 70:30; 65:35; v/v) to collect fractions (Frs. 1–100; 1 mL each). Fraction no. (41–85) were checked on TLC having same R_f 0.51 were pooled into single fraction and it was then dried, purified and recrystallized with methanol. A white amorphous powder (17.14 mg; 0.0114% with respect to GRHA) was obtained and the purity was checked by TLC (benzene:methanol, 7.5:2.5, v/v) on HPTLC pre-coated plates, silica gel 60 F_{254} (Merck, Germany). Using UV light visualization technique (at 254 and 366 nm), the compound 1 (PC) appeared at R_f 0.51 as a fluorescence spot on TLC plates.

2.4. Spectroscopic analysis of isolated compound 1 (PC)

Melting point (m.p. °C) was determined in capillaries by using melting point apparatus (SMP 30, Stuart, UK). UV–Visible spectrophotometric analysis of isolated compound 1 (PC) was carried out (UV 1800, Shimadzu, Japan) with scanning wavelength (200–800 nm). IR spectrum was recorded on KBr pellets using a FT-IR spectrometer (JASCO 410, Tokyo, Japan). ^{1}H NMR, ^{13}C NMR and mass (ESI-HRMS) spectroscopic techniques were used to identify the structure of PC. ^{1}H and ^{13}C NMR spectra (COSY and HMBC) were recorded on Bruker AvIII HD-300 MHz (US) operating at 300 MHz (^{1}H) and 75 MHz (^{13}C), respectively in $CDCl_3$ with TMS as internal standard and chemical shifts were reported in δ units. Mass spectrum was obtained by using Agilent 6520 Q-Tof (US) in ESI (positive mode). Both NMR and mass spectrometry were performed at Sophisticated Analytical Instrumentation Facility, Central Drug Research Institute (CDRI), Lucknow, India. IR spectroscopy was done at Central Instrumentation Facility, Orissa University of Agriculture and Technology (OUAT), Bhubaneswar, Odisha.

2.5. High performance thin layer chromatography (HPTLC)

All analyses were performed with minor modification to the standard method to characterise and validate the isolated compound 1 (PC) in GRHA [7].

2.5.1. Instrumentation

The analysis was performed by using HPTLC pre-coated plate, silica gel aluminium plate 60 F254, (10 cm × 10 cm, 250 mm thickness; Merck, Germany). Samples (GRHA and PC) were sprayed on HPTLC plate by the help of Hamilton syringe sample applicator (Linomat 5, CAMAG, Switzerland) with nitrogen gas flow and were dried on hot plate (TLC Plate Heater 3, CAMAG, Switzerland). Chromatograms were developed in twin trough chamber (20 cm × 10 cm, CAMAG, Switzerland) and densitometry analysis was carried out using scanner (TLC Scanner 4, CAMAG, Switzerland) operated with winCATS planar chromatography manager software (Version 1.14.26, CAMAG, Switzerland). HPTLC analysis was carried out at Central Instrumentation Facility, Orissa University of Agriculture and Technology (OUAT), Bhubaneswar, Odisha.

2.5.2. Chromatographic condition

Samples were prepared in methanol and sprayed on HPTLC plate by using sample applicator. Prior to chromatography development, plates were washed in methanol and activated by drying in a hot plate. Prepared samples were applied on HPTLC plate with a band length of 6 mm, track distance of 10 mm and application positions were 10 mm distance from each side and bottom of the plate. Samples were applied with Linomat V (150 nL/*sec*) under nitrogen gas flow. The chromatogram was developed in twin through chamber with 10 mL of mobile phase consisting of benzene:methanol (7.5:2.5, v/v). Development of the plates were carried out by ascending technique to a migration distance of 90 mm. Detection and densitometry scanning were performed (TLC Scanner 4, CAMAG, Switzerland) in absorption mode at 254 and 366 nm with slit (5 mm × 0.3 mm). Sample track scanning speed was 20 mm/s under control of winCATS planar chromatographic manager software. All analyses were carried out in the laboratory at controlled room temperature (25 ± 3 °C).

2.5.3. Preparation of solutions

2.5.3.1. Standard stock solution. Standard stock solution of compound 1 (PC, 1 mg/mL) and different concentrations of PC (100–500 µg/5 µL) were made in chloroform to obtain final concentration.

2.5.3.2. Validation of method. Validation of the proposed HPTLC method was performed according to the ICH guidelines (ICH, 2005) for the determination of linearity range, precision, sensitivity, specificity, robustness and accuracy of compound 1 (PC) and GRHA.

2.5.3.3. Calibration curve and linearity. Different volumes of PC (100–500 ng/5 µL) were spotted on HPTLC plate to obtain concentration of 100–500 ng/band in triplicate. The peak area versus concentration of PC was plotted. A linear graph was plotted to determine the regression equation (y = mx + c) and r^2.

2.5.3.4. Specificity. The specificity of the method was established by analysing the isolated compound 1 (PC) in GRHA. The presence of PC in GRHA was confirmed by comparing the retardation factor (R_f) and spectra of the developed spots by GRHA. The peak purity of PC was assessed by comparing the start and end position of the spot in appeared bands.

2.5.3.5. Sensitivity (Limit of detection and limit of quantification). Sensitivity study involves both limit of detection (LOD) and limit of quantification (LOQ). For the evaluation of LOD and LOQ, different concentrations of standard solutions of PC were applied along with chloroform as blank and determined on the basis of signal to noise ratio. LOD and LOQ were determined by following formula.

LOD = 3.3 × SD of intercept/Slope (m) and LOQ = 10 × SD of intercept/Slope (m)

2.5.3.6. Precision. As per ICH guidelines, validation of the analytical method was developed for precision. Instrumental precision was measured by replicate (n = 5) applications of PC and expressed as intraday and inter day precision. Intraday assay precision was evaluated by freshly prepared standard solution (100–500 ng/spot) on the same day. Inter day precision was evaluated by applications of PC of the same concentration (100–500 ng/spot) on three different days. The development of peak area due to repeatability of sample application were measured and expressed in terms of % RSD.

2.5.3.7. Accuracy. To validate or check the accuracy of PC, recovery measurements were performed by addition of PC at three different concentration (50, 100 and 150 ng) using the standard addition method. Five replicate experiments were performed to validate the accuracy of PC and values of % recovery for PC were calculated.

2.5.3.8. Robustness. Robustness was performed by varying the selected parameters e.g. mobile phase composition (benzene:methanol; 7.5:2.5, v/v and 8:2, v/v), mobile phase volume (10 ± 5 mL), duration of mobile phase saturation (10 ± 5 min), time of drug application to TLC plate development (10 ± 5 min) and time of TLC plate development to scanning (15 ± 5 min) and there has been no notable alteration found in method performance and results obtained. The effect of these changes on R_f values and peak areas were evaluated by calculating the relative standard deviation for each parameter.

2.6. Antioxidant activities

2.6.1. DPPH free radical scavenging activity of PC

The ability of isolated compound PC to scavenge DPPH free radicals was studied [8]. The antioxidant activity of PC was determined on the basis of its scavenging abilities with the increase in concentration by forming stable DPPHH. About 1 mL of DPPH solution (5.9 mg in 100 mL methanol) was added to 1 mL of different concentrations of GRHA and PC (10–100 μg/mL). After the incubation period of 15–30 min, the absorbance at 517 nm was determined in microplate reader (Synergy H1MF, BioTek, USA). Ascorbic acid was used as a reference drug and % of inhibition was calculated by the following equation

$$\text{Inhibition } (\%) = (A_{Control} \times A_{Sample})/A_{Control} \times 100$$

2.6.2. Cell based antioxidant protection in erythrocytes (CAP-e) assay of PC

CAP-e assay was performed by following methods [6,9]. RBCs (obtained from Wistar rat blood) were prepared by washing twice with sterile normal saline. 1 mg each of GRHA and PC was prepared in 0.9% normal saline (1 mg/mL) at physiological pH and both samples incubated for 20 min, after vortexing. RBC sample was centrifuged at 2400 rpm for 10 min and supernatant was then filtered and kept at −80 °C for assay. RBC was treated with GRHA and PC with different dilutions. Negative controls included samples with no RBCs, whereas RBC with oxidizing agent but not with antioxidant test product was considered as positive control. The oxidative damage caused by the addition of 2,2′-azobis-2-amidinopropane hydrochloride (AAPH) with the decrease in fluorescence of 2′,7′-dichlorofluorescein diacetate (DCF-DA) dye was measured in microplate reader (Synergy H1MF, BioTek, USA). Gallic acid was taken as a reference drug and IC_{50} of PC and GRHA were calculated (g/L).

$$\text{Fluorescence Intensity (FI)} = (FI_{max} - FI_{sample})/(FI_{sample} - FI_{untreated})$$

2.6.3. Oxygen radical absorbance capacity (ORAC) assay of PC

ORAC assay was performed by following methods [6,10]. A stock solution of fluorescein (FL, 5 mM, 150 mL) was prepared in phosphate buffer saline (PBS, 75 mM, pH 7.4) and stored in complete dark under refrigeration conditions. The working solution (80 nM) was prepared freshly by diluting in PBS from the above FL stock solution. 2,2′-azobis (2-methylpropionamidine dihydrochloride) (AAPH, 150 mM) was prepared freshly by dissolving in PBS (10 mM). Trolox (20 μM) was used as reference drug. As ORAC assay is extremely sensitive, GRHA (1 mg/mL) was diluted (30 times) and PC (0.5 mg/mL) was diluted (25 times) to avoid interference. The final reaction mixture was consisting of trolox/GRHA/PC (25 μL) and FL (150 μL). After incubating the reaction mixture for 15–20 min at 37 °C, AAPH was added and fluorescence was recorded (Ex 485 nm and Em 520 nm) at 1 min interval for 70 min in microplate reader (Synergy H1MF, BioTek, USA). The net area under curve (AUC) was calculated by subtracting the AUC of Trolox with AUC of blank. t = 0/fluorescence sample, t = 0 from the normalized curves. The area under curve (AUC) and the net AUC were calculated as follows

$$AUC = 1 + \sum f_i/f_0$$

Net AUC = $AUC_{antioxidant} - AUC_{blank}$ (f_0 was the initial fluorescence reading at 0 min and f_i is the fluorescence reading at time i).

2.7. Cholinesterase inhibition assay of PC

AChE and BChE inhibition activities were calculated by following methods with minor modifications to it [3,11]. ATCI and SBTC substrates were used in AChE and BChE inhibition assays, respectively. DTNB used as the reagent for the measurement of cholinesterase activities. Reaction mixture comprised of DTNB (0.2 mM) in 1 mM sodium phosphate buffer (pH 8.0), test solution e.g. GRHA and PC of 40 μL each in different tubes ranging from 10 to 150 μg. Then enzyme (AChE or BChE, 0.22 U/mL) solutions of 40 μL each were added and incubated at 25 °C for 15 min. The hydrolysis of AChE and BChE were observed by the formation of yellow colour 5-thio-2-nitrobenzoate anions within 15 min. Reactions were performed in triplicate and absorbance was measured at 405 nm by microplate reader (Synergy H1MF, BioTek, USA); where galantamine was considered as reference drug. The concentration of test samples that inhibit the hydrolysis of substrate by 50% (IC_{50}) were determined as a function of increasing concentration of GRHA and PC.

2.8. Mode of cholinesterase inhibition of PC

The mode of inhibition of GRHA and PC towards AChE and BChE was determined [12,13]. Reaction mixture was consisting of AChE (20 μL, 0.22 U/mL), DTNB (1 mL, 3 nM/L) and ATCI (0.05–3 mM/L) in sodium phosphate buffer (0.1 mol/L, pH 8). The final volume was adjusted to 1 mL with 0.1 mol/L sodium phosphate buffer. The mixture was then incubated for 30 min at 25 °C. A double reciprocal (Lineweaver-Burk) plot was plotted between 1/[v] versus 1/[s] to determine the mode of inhibition. The same procedure was followed for BChE inhibition assay in which SBTC was used as substrate. Kinetic values were applied by transforming data to Lineweaver-Burk plot and graphs were plotted in Microsoft Excel (STDEV, 2010) [3].

2.9. Bioautography test of PC

HPTLC based bioautography test was performed [3,14,15]. HPTLC aluminium plates (10 × 10 cm, 0.2 mm thickness) were used for TLC bioassay. GRHA (1 mg/mL in methanol) and PC (1 mg/mL in chloroform) were applied by sample applicator (Linomat V) to plates about 10 mm above the edge using a bandwidth of 6 mm and distance between tracks of 10 mm. Each concentration was spotted on HPTLC plate and the plate was developed by immersing the bottom edge in the developing solvent consisting of an appropriate mobile phase (benzene:methanol; 7.5:2.5, v/v). After developing, the TLC plate was dried and then scanned in TLC scanner 4, CAMAG at 254 and 366 nm. Enzyme inhibitory activities of developed spots were detected by spraying the substrate, dye and enzyme based on Ellman's method [16]. For AChE activities, plates were sprayed with DTNB (1 mM) and ATCI but, in the case of BChE activities, DTNB (1 mM) and SBTC (1 mM) reagent were sprayed until HPTLC plates were saturated with the reagent. It was allowed to dry for 5 min and then appropriate volume of enzyme (3 U/mL) was sprayed. White spots were appeared in yellow background that became visible after few min and persisted for about 10–15 min which indicates the inhibition of cholinesterase enzymes by test samples. The minimum concentration which could be recognized on HPTLC plate was considered as the detection limit and R_f values of respective white spots were noted.

2.10. Molecular modelling and automated docking setup of PC

The X-ray crystal structure of the human and mouse AChE and BChE receptor were obtained from protein data bank (PDB ID: 4M0E-human AChE, 5DTI-mouse AChE and 1P0I-human BChE). Since no crystal structure is available for mouse BChE, a homology model was prepared for the same by using crystal structure of human BChE (PDB-ID 1P0I) with software modeller 9.14. The molecular docking study was performed using Glide module of Schrodinger molecular modelling. Protein structures were prepared for docking using protein preparation wizard by addition of missing side chains and atoms, correction of bond orders, addition of hydrogens and ionisation states etc. The obtained structure was subjected to refinement by energy minimization using the OPLS-2005 force field up to a gradient of 0.01 by fixing heavy atoms. Subsequently, the whole structure was minimized up to a gradient of

0.3 Å. The active site, for the purpose of grid generation, was defined as residues within 5 Å of the co-crystallized ligand. The ligand was drawn by maestro 2D Sketcher and prepared by LigPrep Wizard for the docking using the OPLS-2005 force field. The prepared ligand was docked using extra precision (XP) docking method of Glide module of Schrodinger into the protein structures prepared earlier using default settings [17].

2.11. Statistical analysis

A minimum of five independent experiments were carried and the results were presented as mean ± standard deviation (SD) and standard error mean (SEM) by using Microsoft Excel (STDEV, 2010). Calibration curves of the reference drug were considered to be linear if $r^2 > 0.99$.

3. Results and discussion

3.1. Analysis of isolated compound and structural elucidation of PC

Chromatographic separation was performed and the compound 1 (PC) was isolated as a white amorphous powdered (17.14 mg; 0.0114% with respect to GRHA) which passed the terpene chemical test. Melting point was recorded at 56–57 °C and further, the purity of PC was cross checked by TLC as appeared a single prominent fluorescence spot at R_f 0.51 (benzene:methanol, 7.5:2.5, v/v) at 254 and 366 nm, respectively. UV spectrum with absorbance maxima was recorded ($CHCl_3$), λ_{max} at 266 nm indicated the presence of CH_3-group attached to benzene ring (Fig. 1). The IR spectrum of PC showed the absorbance band of asymmetric C—H stretch (2916.08 cm^{-1}) and symmetric C—H stretch (2848.73 cm^{-1}) for sp^3 hybridised C atom; whereas C=C stretch (1698.84 cm^{-1}) and aromatic C=C stretch (1463.76 cm^{-1}) for sp^2 hybridised C atom. The proton nuclear magnetic resonance (^1H NMR) spectrum of PC was analysed by the aid of ^1H–^1H shift correlated spectroscopy (COSY) and heteronuclear multiple-bond correlation spectroscopy (HMBC). Characteristic signals appeared at δ_H 7.26–7.11 indicating the presence of aromatic protons (Ar*H*) in PC. The presence of CH_3-group attached to benzene ring in PC, showed signal at δ_H 2.34. Three singlet protons in PC appeared at δ_H 1.25 (H-1́, s), 0.90 (1́0-CH_3, s) and 0.92 (H-1́1́, s). Moreover, the presence of olefinic proton and olefinic methyl group signals were appeared at δ_H 2.37 (H-5́, t, J = 7.5 Hz) and 1.63 (6́-CH_3, m). Signals at δ_H 2.32 (H-2́, t, J = 7.5 Hz) and 1.25 (H-1́0, d, J = 13.8 Hz) were due to the presence of two methine protons. Five methylene protons signals appeared at δ_H 1.65 (H-3́, m), 1.68 (H-4́, m), 1.60 (H-7́, m), 1.58 (H-8́, m) and 1.30 (H-9́, d, J = 13.8 Hz). ^{13}C NMR spectrum of PC showed characteristics signals for six aromatic carbons (δ_c 130.18–124.32), five methyl carbons (δ_C 24.93, Ar-CH_3; 22.91, C-1́; 29.90, C-1́1́; 29.81, 1́0-CH_3 and 32.81, 6́-CH_3), two methine carbons (δ_C 77.65, C-2́ and 76.81, C-1́0), five methylene carbons (δ_C 24.93, C-3́; 29.29, C-4́; 29.46, C-7́; 29.58, C-8́ and, 29.66, C-9́) and two olefinic carbons (δ_C 77.44, C-5́ and 77.23, C-6́). The location of aromatic methyl group was confirmed at C-4 by COSY relations of H-3/H(Ar-CH_3), H-5/H(Ar-CH_3) and HMBC relations of H-3/C(Ar-CH_3), H-5/C(Ar-CH_3). The presence of α-methyl group was confirmed at C-2́ by HMBC relations of H-1́/C-1, H-1́/C-6 and H-1́/C-3́. The presence of double bond between C-5 and C-6 was confirmed by COSY relations of H-5́/H-6́ and HMBC relations of H-5́/C-4́, H-5́/C-6́ and H-5́/C(6́-CH_3). Molecular mass of PC was found to be m/z 272.26 $[M + H]^+$ with molecular base peak at m/z 229.03 $[C_{17}H_{25}, 100\%]^+$ and intense fragmentation ion peak at m/z 257.24 $[C_{19}H_{29}, 20\%]^+$, 201.33 $[C_{15}H_{21}]^+$, 187.3 $[C_{14}H_{19}]^+$, 147.24 $[C_{11}H_{15}]^+$, 133.21 $[C_{10}H_{13}]^+$, 91.13 $[C_7H_7]^+$ by ESI-HRMS (positive mode) (Table 1A). Based on earlier report on its presence in *G. repens* and structural elucidation by spectroscopic studies confirmed that the isolated molecule (PC) was 1-(6′,10′-dimethylundec-5′-en-2′α-yl)-4-methylbenzene or Pentylcurcumene (Fig. 1) [18].

3.2. HPTLC study of Pentylcurcumene (PC)

HPTLC is an efficient and routine analytical technique to analyse the drug sample in nanogram (ng) level. This technique is widely accepted by researchers due to its sensitivity, less time consuming and cost effectiveness [7].

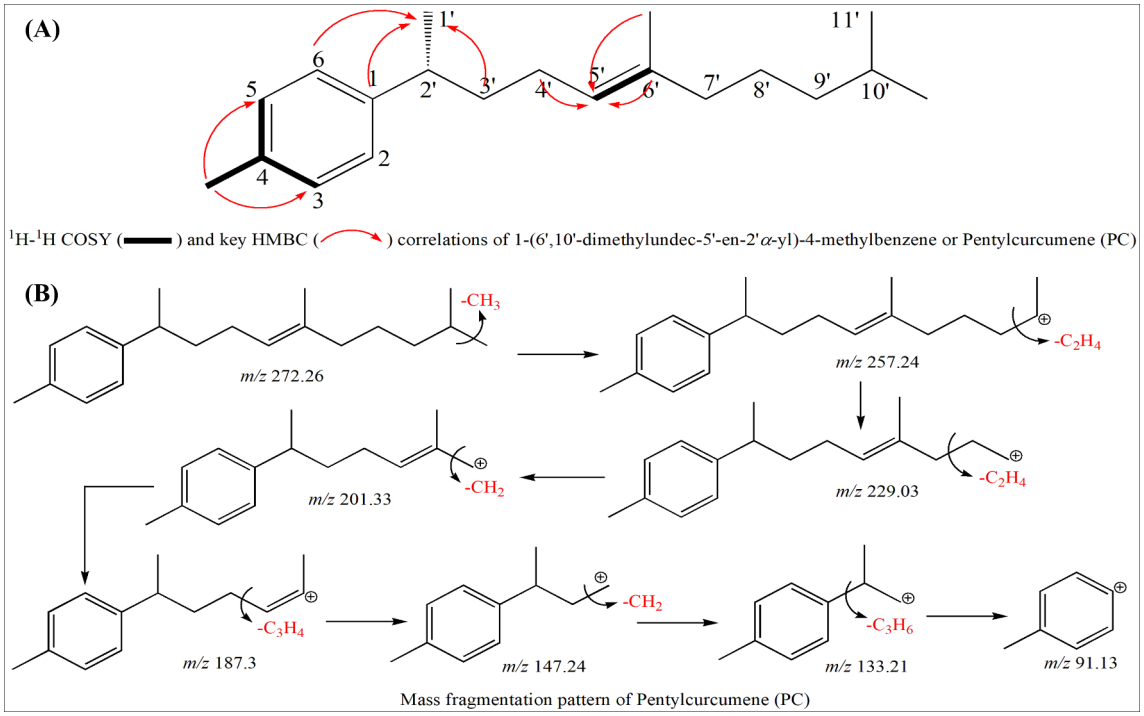

Fig. 1. Structure and mass fragmentation pattern of Pentylcurcumene (PC). Fig. A represents structure of Pentylcurcumene (PC) with COSY and HMBC correlations. Fig. B represents mass fragmentation pattern of Pentylcurcumene (PC).

Table 1
Melting point, spectroscopic analysis and molecular docking study of the compound.

Parameter	Experimental data
(A) Spectroscopic analysis data	
Melting point	56–57 °C
UV (λ_{max}) ($CHCl_3$)	214, 241, 266 ($C_6H_5-CH_3$) nm
IR (KBr, ν_{max} cm^{-1})	2916.08 (C−$H_{asymmetric\ stretch}$), 2848.73 (C−$H_{symmetric\ stretch}$), 1698.84 (C=$C_{stretch}$), 1463.76 (aromatic C=$C_{stretch}$)
ESI-HRMS (Positive mode)	*m/z* 272.26 $[M+H]^+$, 257.24 $[C_{19}H_{29}]^+$, 229.03 $[C_{17}H_{25}]^+$, 201.33 $[C_{15}H_{21}]^+$, 187.3 $[C_{14}H_{19}]^+$, 147.24 $[C_{11}H_{15}]^+$, 133.21 $[C_{10}H_{13}]^+$, 91.13 $[C_7H_7]^+$
^{1}H NMR	^{1}H NMR ($CDCl_3$, 300 MHz): δ_H 7.26–7.11 (4H, Ar*H*), 2.34 (3H, $ArCH_3$), 1.25 (3H, s, CH_3), 2.32 (1H, t, *J* = 7.5 Hz, CH), 1.68–1.58 (8H, m, $4CH_2$), 2.37 (1H, t, *J* = 7.5 Hz, CH), 1.63 (3H, m, CH_3), 1.30 (2H, d, *J* = 13.8 Hz, CH_2), 1.25 (1H, d, *J* = 13.8 Hz, CH), 0.90 (3H, s, CH_3), 0.92 (3H, s, CH_3)
^{13}C NMR	^{13}C NMR ($CDCl_3$, 75 MHz): δ_C 130.18 (C), 129.41 (C), 128.12 (CH), 126.14 (CH × 2), 124.32 (CH), 77.65 (CH), 77.44 (CH), 77.23 (C), 76.81 (CH), 32.81 (CH_3), 29.90 (CH_3), 29.81 (CH_3), 29.66 (CH_2), 29.58 (CH_2), 29.46 (CH_2), 29.29 (CH_2), 24.93 (CH_2), 24.93 (Ar-CH_3), 22.91 (CH_3)
Formula	$C_{20}H_{32}$

Species	Receptor	PDB-ID	Docking Score
(B) Molecular docking of Pentylcurcumene (PC)			
Human	AChE(H)	4M0E	−5.6
Mouse	AChE(M)	5DTI	−6.1
Human	BChE(H)	1P0I	−6.9
Mouse	BChE(M)	Homology model	−4.18

UV–Visible, IR, ^{1}HNMR, ^{13}CNMR and Mass spectroscopy analysis of isolated molecule Pentylcurcumene (PC). Molecular docking scores of Pentylcurcumene (PC) as ligand towards acetylcholinesterase (AChE; human/rat) and butyrylcholinesterase (BChE; human/rat) were analysed and protein structures were obtained from protein data bank (http://www.rcsb.org).

3.2.1. Optimization of HPTLC chromatographic conditions

Different solvent compositions (eluents) were performed to achieve better separation and resolution of bands of GRHA and PC on HPTLC pre-coated plate (silica gel aluminium plate 60 F254). Optimization of chromatographic separations was achieved with the eluent benzene:-methanol (7.5:2.5, v/v) and the fingerprint patterns were quantitated accurately by recording R_f values of isolated drug PC 0.50 ± 0.04 and 0.51 ± 0.05 at 254 nm and 366 nm, respectively (Fig. 2A and F). From the chemical chromatographic patterns (post derivatisation), PC passed the terpene chemical test and further validated by HPTLC techniques (Table 2).

3.2.2. Calibration curves and linearity

Calibration curve was constructed by plotting peak area and concentration of PC (Fig. 2E and J) and the linear regression analysis data was obtained from the calibration plots, displayed good linear relationship with respect to peak height and peak area of PC over the concentration range 100–500 ng/spot (Table 2). No significant difference was observed between the regression coefficient values (r^2) 0.9977 and 0.9983 at UV/254 nm and Vis/366 nm, respectively.

3.2.3. Specificity

The specificity of the method was ascertained by peak purity profiling studies. Purity of the isolated drug (PC) peak was ascertained by

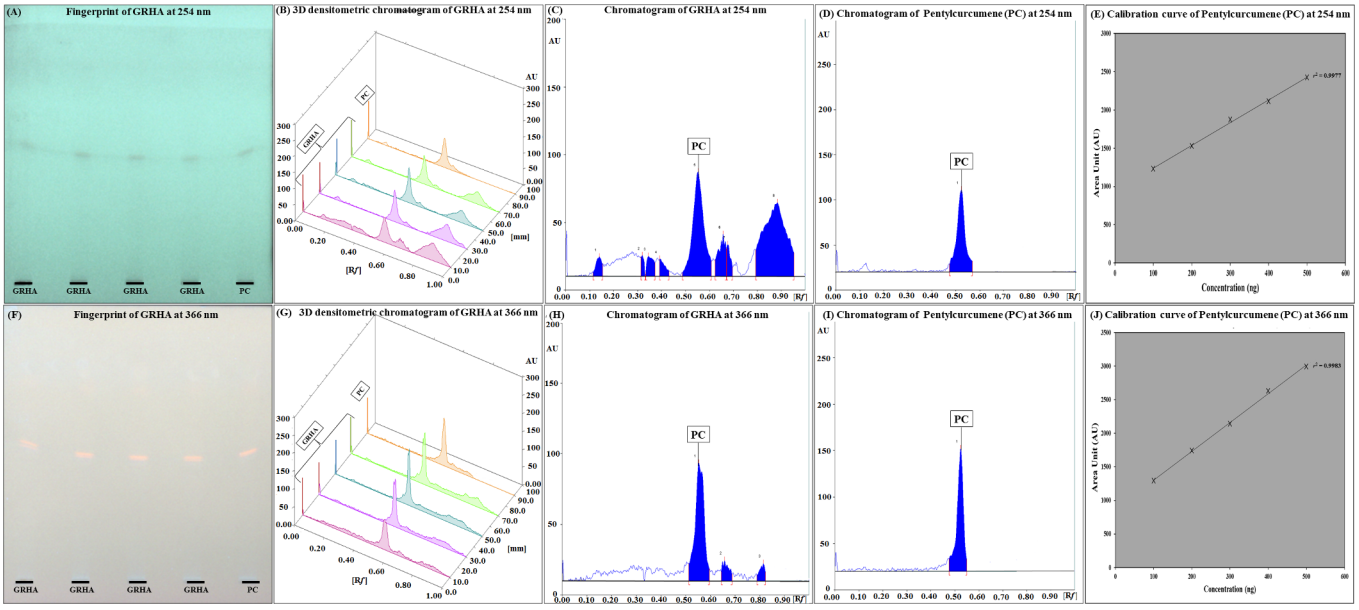

Fig. 2. HPTLC analysis of hydroalcohol extract of *Geophila repens* (GRHA), ranging from 100, 200, 300, 400 ng/spot and Pentylcurcumene (PC; 100 ng/spot) at 254 and 366 nm. Figs. A and F represents the fingerprint of GRHA and Pentylcurcumene (PC). Figs. B and G represents the 3D densitometric chromatogram of GRHA and Pentylcurcumene (PC). Figs. C and H represents the chromatogram of GRHA shows the presence of Pentylcurcumene (PC), with R_f 0.50 and 0.51 at 254 and 366 nm, respectively. Figs. D and I represent the reported single peak of Pentylcurcumene (PC) with R_f 0.50 and 0.51 (Benzene:methanol: 7.5:2.5 v/v) recorded at 254 and 366 nm, respectively. Figs. E and J represent the calibration curve of Pentylcurcumene (PC) at 254 and 366 nm with r^2 values of 0.9977 and 0.9983, respectively.

Table 2
Linear regression analysis data of HPTLC calibration curve of Pentylcurcumene (PC).

Parameter	Values	
	At 254 nm	At 366 nm
R_f	0.50	0.51
Specificity	Specific	Specific
Linearity range (ng band^{-1})	100–500 ng	100–500 ng
Regression equation	y = 2.9723x + 941.72	y = 4.2894x + 872.9
Correlation coefficient (r^2)	0.9977	0.9983
LOD	16.13 ng	13.48 ng
LOQ	48.88 ng	31.429 ng
Inter day precession (% RSD)	0.414–1.01	0.519–1.225
Intraday precession (% RSD)	0.591–1.528	0.466–1.188
% recovery	97.17–98.71	90.53–97.36
Robustness	Robust	Robust

Linear regression equation, correlation coefficient, limit of detection (LOD) and limit of quantification (LOQ) values of Pentylcurcumene (PC) at 254 and 366 nm, respectively.

analysing the spectrum at peak start, middle and at peak end. Optimisation of chromatographic separations of GRHA was achieved with the mobile phase e.g. benzene:methanol (7.5:2.5, v/v) and the peak with R_f values 0.50 at 254 nm and 0.51 at 366 nm were matched exactly with the corresponding R_f values of PC (0.50 at 254 nm and 0.51 at 366 nm). The results obtained by the proposed method showed that there were no interfering bands and impurity within same R_f values of GRHA (Fig. 2A-D and F-I).

3.2.4. Sensitivity

Detection limit and quantification limit were calculated by respective standard deviation and slope at 254 and 366 nm of calibration curve (Fig. 2E and J). LOD of PC was found to be 16.13 and 13.48 ng/spot at 254 nm and 366 nm, whereas LOQ of PC was found to be 48.88 and 31.429 ng/spot at 254 nm and 366 nm, respectively (Table 2). The method was sufficiently sensitive for a precise determination at nanogram level.

3.2.5. Precision

The experiment study was repeated three times in one day (intraday precision) and the average % relative standard deviation (% RSD) were calculated. Also, the experiment was repeated on three different day (inter day precision) and the average % RSD for the peak areas of PC was calculated. % RSD values for intraday and inter day variation of PC at five different concentration levels (100–500 ng/spot) are given in Table 3A and found that the values were less than 2 of inter day (0.506–1.01 and 0.519–1.225) and intraday (0.591–1.528 and 0.494–1.188) at 254 nm and 366 nm, respectively. The low % RSD values (≤ 2) indicated that the method was precise and accurate.

3.2.6. Accuracy

The amount of PC in GRHA was found to be 8.92 ng and 9.79 ng at 254 nm and 366 nm, respectively. However, the accuracy method was validated by standard addition of PC at 3 different concentrations (50, 100 and 150 ng) in GRHA. The mean % recoveries after spiking were found in the range of 97.17–98.71 % (at 254 nm) and 90.53–97.36% (at 366 nm); indicates the method is accurate (Table 3B).

3.2.7. Robustness

The minor modification in original mobile phase composition with new conditions by different trail of mobile phase volume, sample application time and scanning time; the robustness of PC was varied slightly on the basis of its R_f values e.g. 0.50 ± 0.25 at 254 nm and 0.51 ± 0.25 at 366 nm, respectively. The % RSD values for peak area (≤ 3) indicated the highly robust nature of the developed method (Table 3C).

3.3. Antioxidant studies of Pentylcurcumene (PC)

3.3.1. DPPH free radical scavenging activity

Antiradical scavenging activity of Pentylcurcumene (PC) was tested by the DPPH model. The assay is based on the activity of hydrogen atom donating ability of PC on DPPH (free radical generator) to form stable DPPHH [3,19]. IC_{50} values of GRHA and PC were recorded 41.76 ± 1.04 and 86.08 ± 2.56 μg/mL, respectively, whereas the IC_{50} of reference drug ascorbic acid was 33.10 ± 1.04 μg/mL (Fig. 3A). The obtained results therefore suggest that the presence of higher content of phenolic, flavonoid and PC were responsible for antioxidant effects of GRHA which act synergistically by donating hydrogens to free radicals

Table 3
Precision, accuracy and robustness study of Pentylcurcumene (PC).

Concentration (ng/spot)	Inter day precision (n = 5)		Intraday precision (n = 5)	
	Mean area ± SD	% RSD	Mean area ± SD	% RSD
(A) Inter day and intraday precision study for Pentylcurcumene (PC)				
At 254 nm				
100	1236.20 ± 12.51	1.01	1198.61 ± 18.32	1.528
200	1587.19 ± 11.80	0.746	1539.08 ± 15.09	0.980
300	1892.09 ± 14.26	0.753	1852.49 ± 17.19	0.927
400	2154.26 ± 10.03	0.466	2109.63 ± 13.71	0.649
500	2459.31 ± 12.49	0.506	2401.60 ± 14.20	0.591
At 366 nm				
100	1309.98 ± 16.05	1.225	1299.98 ± 15.45	1.188
200	1765.03 ± 13.15	0.745	1755.03 ± 14.65	0.834
300	2176.54 ± 14.71	0.675	2169.54 ± 13.01	0.599
400	2673.98 ± 13.95	0.521	2665.98 ± 11.05	0.414
500	3012.80 ± 15.65	0.519	3002.80 ± 14.85	0.494

Sample	Quantity of sample (ng)	Amount of PC found in A (ng)	Amount PC added to A (ng)	Total amount B+C (ng)	Total PC found (ng)	% of recovery (Mean ± SD)
	A		B		C	
(B) Accuracy study of Pentylcurcumene (PC) in *G. repens*						
At 254 nm						
GRHA	500	8.45	50	58.45	56.80	97.17 ± 0.653
	500	8.92	100	108.92	106.48	97.75 ± 0.612
	500	8.06	150	158.06	156.03	98.71 ± 0.530
At 366 nm						
GRHA	500	9.50	50	59.50	53.87	90.53 ± 0.782
	500	9.01	100	109.01	105.76	97.01 ± 0.614
	500	9.79	150	159.79	155.58	97.36 ± 0.527

Parameters	At 254 nm		At 366 nm	
	% mean recovery ± SD	% RSD	% mean recovery ± SD	% RSD
(C) Robustness study of Pentylcurcumene (PC)				
Mobile phase composition (Benzene:methanol; 7.5:2.5 v/v and 8:2 v/v)	97.26 ± 2.17 96.16 ± 2.11	2.231 2.194	97.56 ± 2.87 96.50 ± 1.85	2.941 1.917
Mobile phase (10 ± 5 mL)	97.94 ± 1.42	1.449	98.54 ± 2.32	2.354
Chamber saturation time (10 ± 5 min)	98.49 ± 1.52	1.543	99.89 ± 0.92	0.921
Time of HPTLC development (10 ± 5 min)	96.89 ± 1.09	1.124	97.49 ± 0.72	0.738
Time of HPTLC scanning (15 ± 5 min)	98.53 ± 2.39	2.425	99.13 ± 2.49	2.511

Precision (Intraday and inter day), accuracy and robustness values of Pentylcurcumene (PC) at 254 and 366 nm, respectively.

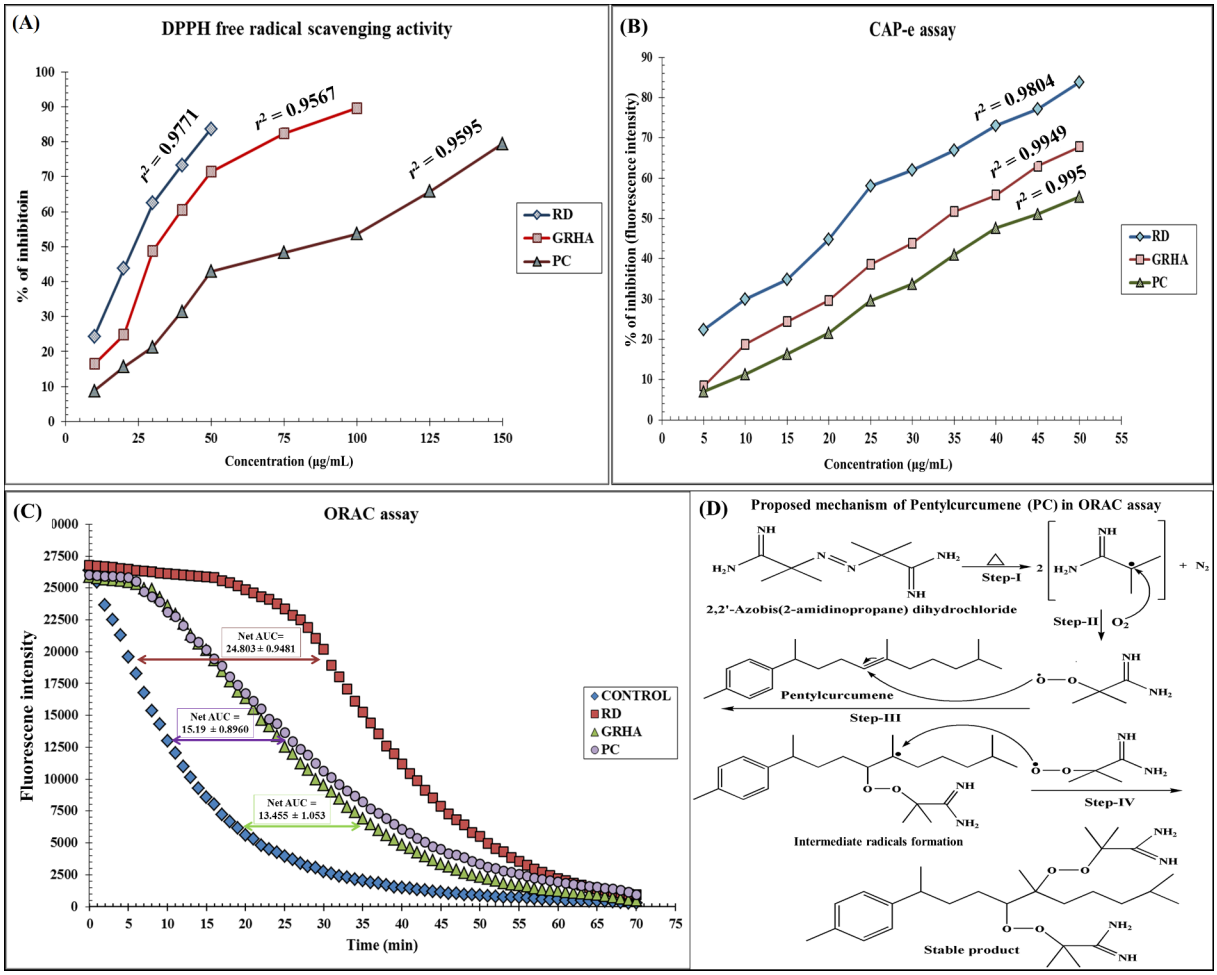

Fig. 3. Free radical scavenging and cellular antioxidant activities of hydroalcohol extract of *Geophila repens* (GRHA) and Pentylcurcumene (PC). Fig. A represents DPPH assay of GRHA and PC with their respective IC_{50} values 41.76 ± 1.04 and 86.08 ± 2.56 µg/mL, whereas ascorbic acid (33.10 ± 1.04 µg/mL) was considered as a reference drug (RD). Fig. B represents % of inhibition of cell-based antioxidant protection in erythrocytes (CAP-e) assays of GRHA and PC with IC_{50} values 35.03 ± 0.6952 and 43.92 ± 0.8732 µg/mL, respectively which were comparable with reference drug gallic acid (23.69 ± 0.4903 µg/mL). Fig. C shows the area under curve (AUC) in oxygen radical absorbance capacity (ORAC) assay of GRHA and PC with net AUC 13.455 ± 1.053 and 15.19 ± 0.8960, respectively and comparable with trolox (24.803 ± 0.9481) as reference drug. Fig. D depicts the proposed reaction mechanism of 2,2′-azobis (2-methylpropionamidine dihydrochloridc)/AAPH which generates free radical upon heat and reacts with Pentylcurcumene by forming intermediate radicals and reaction mechanism ends with the formation of stable product.

to inhibit or interrupting the formation and propagation of free radicals [3]. However, free radical scavenging activity of PC was attributed to its ability to donate allylic hydrogen to DPPH˙ radical to form resonance stabilised compound and it may be embraced as therapeutic agent in free radical induced neurological disorder.

3.3.2. Cell based antioxidant protection in erythrocytes (CAP-e) assay

The assay was performed in erythrocytes (RBC model from rat) to evaluate the antioxidant capacity of Pentylcurcumene (PC) in living system. RBC model was chosen because it is simple and RBC does not produce ROS or undergo apoptosis. The decrease in fluorescent intensity of DCF-DA (fluorescent probe) in the presence of peroxy radical generator AAPH marked the cellular protection ability of GRHA and PC in RBC [6]. The antioxidant potential of GRHA and PC in terms of IC_{50} values reported at 35.03 ± 0.69 and 43.92 ± 0.87 µg/mL, respectively and both results were comparable to the reference drug gallic acid (23.69 ± 0.49 µg/mL) (Fig. 3B). Pentylcurcumene (PC) plays an important role in the protection of cellular membranes and lipoproteins against intracellular ROS produced by peroxyl radicals as these radicals can damage to lipids in the cell wall. The long unsaturated alkyl chains in Pentylcurcumene (PC) are highly lipophilic in nature and it deactivates the peroxyl radicals by reacting with them to form resonance stabilized carbon-centered radical adducts and disrupts the reaction sequence and prevents the damage to cellular lipids [20,21].

3.3.3. Oxygen radical absorbance capacity (ORAC) assay

The antioxidant potential of Pentylcurcumene (PC) was evaluated by ORAC assay that relies on fluorescence quenching effect of antioxidants. ORAC reaction is highly sensitive and allows limit of detection (LOD) lower than nM. It is based on *in situ* production of peroxy free radicals by AAPH that are able to react with substrate resulting in change in fluorescent intensity (FI) and increase in the rate of fluorescent decay. Quantification of scavenging potential of GRHA and PC towards peroxyl radicals were evaluated in terms of net area under curve (AUC). Antioxidant protections were calculated by subtracting resultant AUC. AUC of GRHA and PC were 13.45 ± 1.05 and 15.19 ± 0.89, respectively. Both results were found comparable to Trolox 24.80 ± 0.94 (Fig. 3C). PC showed good peroxyl radical scavenging activity [6,22]. The reaction mechanism describes the step by step sequence of reactions of PC towards the ability to scavenge peroxyl radical (generated by thermolysis of AAPH) by which the chemiluminescence intensity of fluorescein sodium was reduced. In the proposed reaction mechanism (Fig. 3D), AAPH undergoes thermal decomposition to form two amidinopropane radicals which reacts with O_2

to produce peroxy amidinopropane radicals. Then peroxy amidinopropane radicals reacted with fluorescein sodium and exhibited maximum FI. The peroxy radical scavenging activity was determined with the decrease in FI caused by PC as it reacts (at C-5́ and C-6́) with peroxy amidinopropane radicals to form stable product (5́,6́-di-peroxy amidinopropyl pentylcurcumene).

Oxidative stress is believed to play a role in aging and neurodegenerative diseases. The previous report of antioxidant activity of *G. repens* is thus supported with result of the current investigation of Pentylcurcumene made through DPPH, CAP-e and ORAC assays [3]. It may therefore be claimed that the species contains important antioxidant principles like Pentylcurcumene that contribute to neuroprotective activities.

3.4. Cholinesterase inhibition activities of Pentylcurcumene (PC)

The current investigation demonstrated acetylcholinesterase (AChE) and butyrylcholinesterase (BChE) inhibitory activities of PC. In AChE inhibitory activities, IC_{50} of GRHA and PC were 65.96 ± 0.43 and 73.12 ± 0.56 µg/mL whereas, in BChE inhibitory activities, IC_{50} of GRHA and PC were recorded 86.03 ± 0.47 and 97.65 ± 0.46 µg/mL, respectively. In both assays, IC_{50} of galantamine was recorded 26.34 ± 0.45 (AChE inhibition) and 28.35 ± 0.43 µg/mL (BChE inhibition) (Fig. 4A and D). Results suggest that Pentylcurcumene in *G. repens* is a first-line cholinesterase inhibitor may be relevant in slowing AD progression due to its effective radical scavenging activities [23,24].

3.5. Mode of inhibition of Pentylcurcumene (PC)

Enzyme kinetics of PC as AChE and BChE inhibitor was performed in the form of double reciprocal (Lineweaver-Burk) plot against 1/[s] versus 1/[v] (where 's' is substrate concentration and 'v' is reaction velocity). After analysing mode of inhibition from the plot with graphical analytic tool, the nature of AChE and BChE inhibition caused by both GRHA and PC showed reversible competitive inhibition as evidenced by intersection at Y-axis with V_{max} 0.8 and 0.6, respectively (Fig. 4B and E). Our findings and the mechanism of inhibition specifies that GRHA and PC have competed at the active sites on AChE and BChE surface by blocking the substrates (ATCI and SBTC) binding on both enzymes, respectively which are in full agreement with results achieved in the present study [3].

3.6. Bioautography test of Pentylcurcumene (PC)

HPTLC bioautography tests were performed to identify the cholinesterase inhibitory effect of bioactive principles present in GRHA. It is a simple and less time-consuming process to detect the anticholinesterase activities of PC at nanogram level. Experimental evidences of our earlier work on HPTLC bioautographic test shows the localization of bioactivity molecules on R_f range 0.42–0.58 were responsible for anticholinesterase activities [3]. Earlier application of bioautography test has led to the target-directed isolation of bioactive compound e.g. Pentylcurcumene (PC). The fingerprint of GRHA (Track

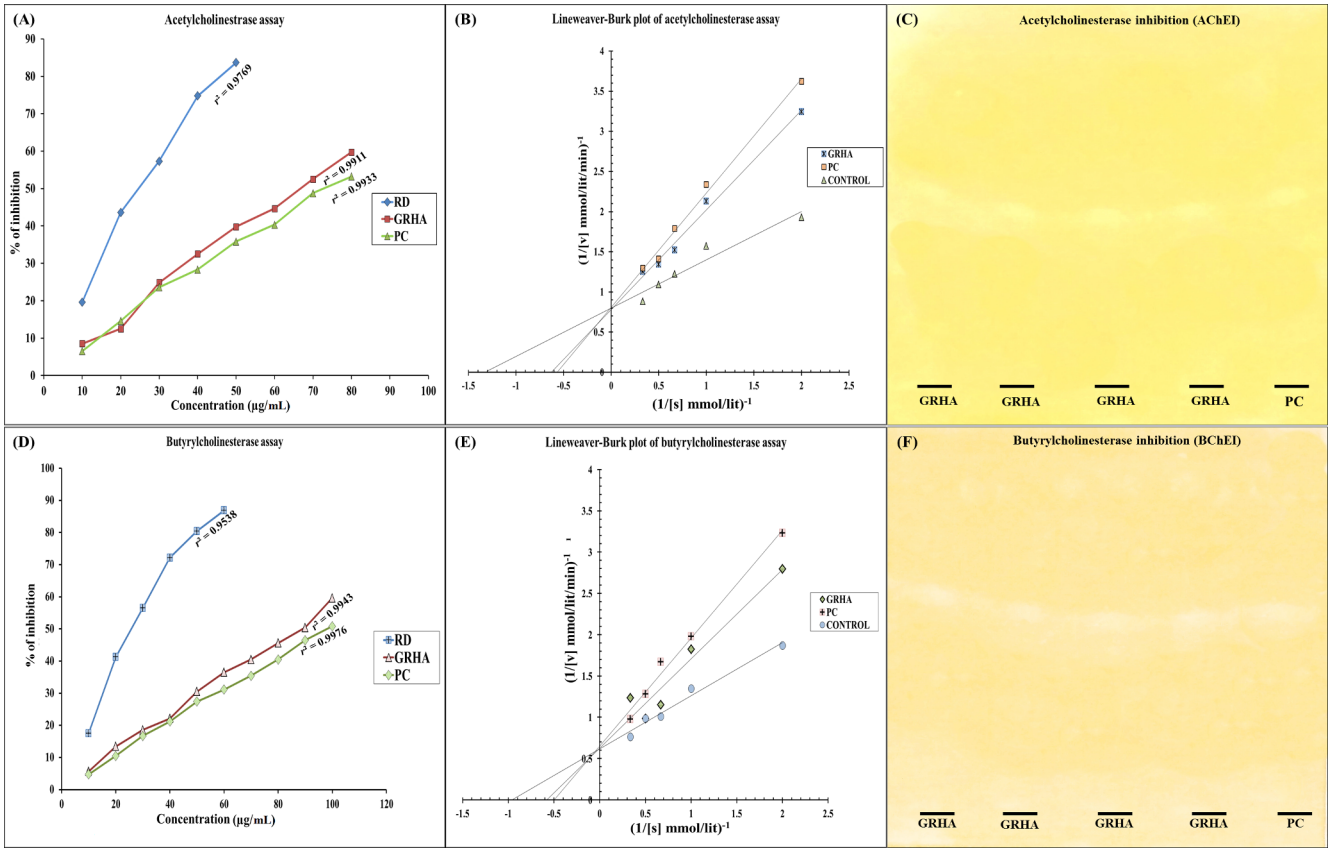

Fig. 4. Anticholinesterase, mode of inhibition and HPTLC bioautography test of hydroalcohol extract of *Geophila repens* (GRHA) and Pentylcurcumene (PC). Fig. A represents acetylcholinesterase (AChE) inhibitory activity of GRHA and Pentylcurcumene (PC) with IC_{50} 65.96 ± 0.439 and 73.12 + 0.564 µg/mL, respectively and Fig. D represents butyrylcholinesterase (BChE) inhibitory activity of GRHA and Pentylcurcumene (PC) with IC_{50} 86.039 ± 0.470 and 97.65 ± 0.465 µg/mL, respectively. The reference drug galantamine with IC_{50} 26.34 ± 0.459 and 28.35 ± 0.434 µg/mL were recorded in AChE and BChE inhibition studies. Figs. B and E represent the mode of inhibition of AChE and BChE activity by plotting Lineweaver-Burk plot with V_{mx} 0.8 (approx.) and 0.6 (approx.), respectively in a different substrate concentrations (0.05–3 mmol/lit) which signifies competitive inhibition (reversible) in the presence of GRHA and Pentylcurcumene (PC). Figs. C and F depicts the HPTLC bioautography test of AChE and BChE inhibition of GRHA and Pentylcurcumene (PC) as inhibitions were visible with appearance of white spots at R_f 0.50–0.51 (Benzene:methanol; 7.5:2.5 v/v) in yellow background.

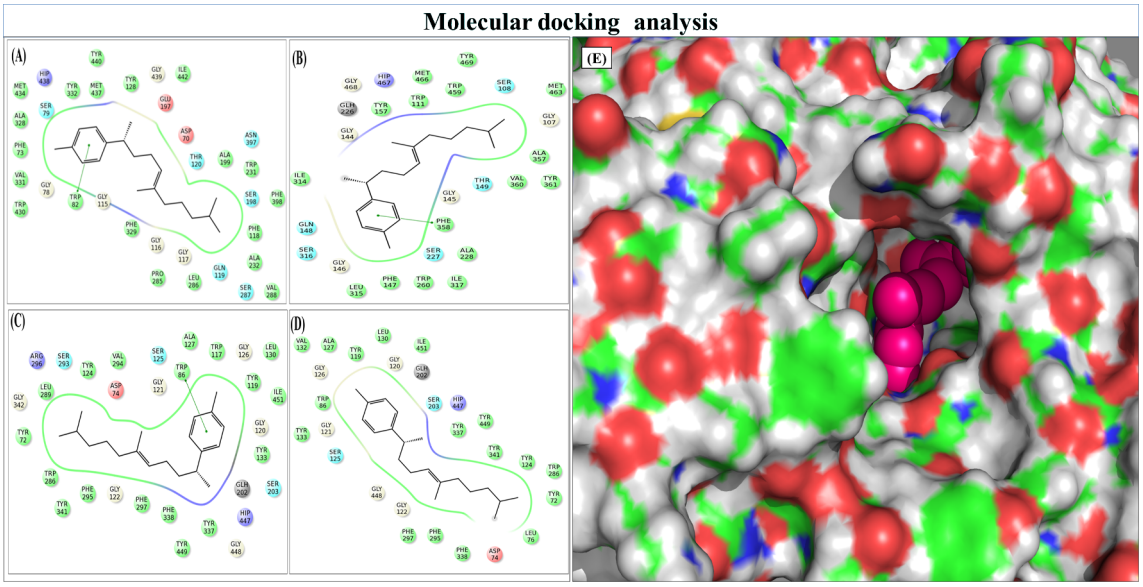

Fig. 5. Molecular docking analysis of cholinesterase enzyme (A) acetylcholinesterase (human), (B) acetylcholinesterase (mouse), (C) butyrylcholinesterase (human) and (D) butyrylcholinesterase (mouse) with protein-Pentylcurcumene (PC) interaction (π-π) and (E) showing the binding of drug at active sites of the targeted protein. The ligand is shown in pink spheres while the protein surface is coloured according to atoms, (carbon-green, hydrogen-white, oxygen-red, nitrogen-blue).

1–4; 100–400 ng) and PC (Track 5; 100 ng) were developed (benzene:methanol; 7.5:2.5, v/v) on HPTLC pre-coated plates, silica gel 60 F_{254} (Merck, Germany) and R_f values were recorded 0.51 at 254 nm and 366 nm, respectively. On AChE and BChE inhibition plates, ATCI and SBTC substrates were treated, respectively. After 10–15 min of substrate and enzyme treatment on plates, white spots were visible clearly at R_f 0.51, with yellow background on both plates (Fig. 4C and F). The study resulted in a successful implementation of bioautography detection method as an improved and advanced HPTLC tool for Pentylcurcumene towards acetylcholinesterase (AChE) and butyrylcholinesterase (BChE) inhibition activities.

3.7. Molecular docking analysis of Pentylcurcumene (PC)

In order to correlate with *in vitro* experimental results, computational tool of molecular docking studies was performed to explore the possible binding interaction of Pentylcurcumene (PC) with active sites of AChE (human/mouse) and BChE (human/mouse). Pentylcurcumene (PC) was docked by using Glide module of Schrodinger molecular modelling with docking scores −5.6, −6.1, −6.9, and −4.18 for hAChE, mAChE, hBChE and mBChE, respectively (Table 1B). The docking results showed that the 2D plot of protein-ligand interaction was within 5 Å and ligand was docked pretty well for both BChE (human) and AChE (human and mouse). A close look of Fig. 5A-D showed that the ligand binds in a hydrophobic cavity lined by hydrophobic residues and aryl ring made π-π interactions with the aromatic rings of Trp82 (AChE-human), Phe358 (AChE-mouse), Trp86 (BChE-human). The hydrophobic tail of the molecule is buried in the hydrophobic core of the residues Trp, Phe, Tyr, Leu and Val etc. The binding of ligand with protein as shown in Fig. 5E and it was clearly visible that the ligand fits in the active sites of protein by well occupying the whole active sites. The molecular docking results support anticholinesterase activities of Pentylcurcumene (PC) with good agreement towards Alzheimer's disease (AD) [25].

4. Conclusion

Based on results of our current findings, it is concluded that Pentylcurcumene, a terpene is an important bioactive molecule in *G. repens* has potential anticholinesterase activities and it could be a potential source of drug in Alzheimer's disease (AD). The molecular docking results support anticholinesterase activities of Pentylcurcumene with good agreement towards Alzheimer's disease. An improved and advanced HPTLC tool resulted in a successful implementation of bioautography detection method of Pentylcurcumene in *G. repens* towards acetylcholinesterase (AChE) and butyrylcholinesterase (BChE) inhibition activities. Bioautography method will be extremely helpful in the identification of other novel anticholinesterase compounds in *G. repens*. HPTLC densitometric method was developed for the analysis of Pentylcurcumene (PC) in *G. repens* and was validated in accordance with the requirements of ICH guidelines and proved to be repeatable, precise, accurate and robust. The procedure is simple, rapid and inexpensive in comparison with other analytical methods. Further investigations are to be needed in *in vivo* model to establish the key mechanism and establish the proper pathway of Pentylcurcumene to combat neurological diseases like Alzheimer's disease.

Conflict of interest

We declare that we have no conflict of interest.

Acknowledgments

Financial support for this work was provided by Forest & Environment Department, Govt. of Odisha, Bhubaneswar (Grant no. R& D-22/18).

The authors wish to acknowledge Central Drug Research Institute, Lucknow, India for spectroscopic analysis and Central Instrumentation Facility, Orissa University of Agriculture and Technology, Bhubaneswar, India for HPTLC studies.

The authors wish to thank Dr. P.C. Panda, Principal Scientist (Taxonomy and Conservation), Regional Plant Resource Centre, Bhubaneswar, India for identification of *Geophila repens*.

Appendix A. Supplementary material

Supplementary data to this article can be found online at https://doi.org/10.1016/j.bioorg.2019.102947.

References

[1] A.K. Sahoo, J. Dandapat, U.C. Dash, S. Kanhar, Features and outcomes of drugs for combination therapy as multi-targets strategy to combat Alzheimer's disease, J. Ethnopharmacol. 215 (2018) 42–73.

[2] X. Wang, W. Wang, L. Li, G. Perry, H. Lee, X. Zhu, Oxidative stress and mitochondrial dysfunction in Alzheimer's disease, Biochim. Biophys. Acta. 2014 (1842) 1240–1247.

[3] U.C. Dash, A.K. Sahoo, *In vitro* antioxidant assessment and a rapid HPTLC bioautographic method for the detection of anticholinesterase inhibitory activity of *Geophila repens*, J. Integr. Med. 15 (2017) 231–241.

[4] A.M.S. Guaqueta, E. Osorio, G.P.C. Gomez, Linalool reverses neuropathological and behavioural impairments in old triple transgenic Alzheimer's mice, Neuropharmacology 102 (2016) 111–120.

[5] A.E. Bianchini, Q.I. Garlet, J.A. da Cunha, G. Bandeira, I.C.M. Brusque, J. Salbego, B.M. Heinzmann, B. Baldisserotto, Monoterpenoids (thymol, carvacrol and S-(+)-linalool) with anesthetic activity in silver catfish (*Rhamdia quelen*): evaluation of acetylcholinesterase and GABAergic activity, Braz. J. Med. Biol. Res. 50 (2017) e6346.

[6] S. Kanhar, A.K. Sahoo, A.K. Mahapatra, The ameliorative effect of *Homalium nepalense* on carbon tetrachloride-induced hepatocellular injury in rats, Biomed. Pharmacother. 103 (2018) 903–914.

[7] S. Gautam, V.K. Shukla, R. Ukawala, G. Gampa, R.N. Saha, Development of a new, rapid and sensitive HPTLC method for estimation of Milnacipran in bulk, formulation and compatibility study, Arab. J. Chem. 10 (2017) 2417–2423.

[8] A.K. Mahapatra, S.S. Pani, A.K. Sahoo, Free radical-scavenging activities of *Homalium* species-an endangered medicinal plant of Eastern Ghats of India, Nat. Prod. Res. 29 (2015) 2112–2116.

[9] D. Honzel, S.G. Carter, K.A. Redman, A.G. Schauss, J.R. Endres, G.S. Jensen, Comparison of chemical and cell-based antioxidant methods for evaluation of foods and natural products: generating multifaceted data by parallel testing using erythrocytes and polymorphonuclear cells, J. Agric. Food. Chem. 56 (2008) 8319–8325.

[10] K. Thaipong, U. Boonprakob, K. Crosby, L. Cisneroszevallos, B.D. Hawkins, Comparison of ABTS, DPPH, FRAP, and ORAC assays for estimating antioxidant activity from guava fruit extracts, J. Food Compost. Anal. 19 (2006) 669–675.

[11] E.A. Adewusi, V. Steenkamp, *In vitro* screening for acetylcholinesterase inhibition and antioxidant activity of medicinal plants from southern Africa, Asian Pac. J. Trop. Med. 4 (2011) 829–835.

[12] D.L. Nelson, M.M. Cox, Lehninger Principles of Biochemistry, New York, 2008.

[13] M. Benabent, E. Vilanova, M.Á. Sogorb, J. Estevez, Cholinesterase assay by an efficient fixed time endpoint method, MethodsX 1 (2014) 258–263.

[14] A. Marston, J. Kissling, K. Hostettmann, A rapid TLC bioautographic method for the detection of acetylcholinesterase and butyrylcholinesterase inhibitors in plants, Phytochem. Anal. 13 (2002) 51–54.

[15] M.K. Dalai, S. Bhadra, S.K. Chaudhary, A. Bandyopadhyay, P.K. Mukherjee, Anticholinesterase activity of the standardized extract of *Syzygium aromaticum* L, Pharmacogn. Mag. 10 (2014) 276–282.

[16] G.L. Ellman, K.D. Courtney, V.J. Andres, R.M. Feather-stone, A new and rapid colorimetric determination of acetylcholinesterase activity, Biochem. Pharmacol. 7 (1961) 88–95.

[17] R.A. Friesner, R.B. Murphy, M.P. Repasky, L.L. Frye, J.R. Greenwood, T.A. Halgren, P.C. Sanschagrin, D.T. Mainz, Extra precision Glide: docking and scoring incorporating a model of hydrophobic enclosure for protein-ligand complexes, J. Med. Chem. 49 (2006) 6177–6196.

[18] H. Rao, P. Lai, Y. Gao, Chemical composition, antibacterial activity, and synergistic effects with conventional antibiotics and nitric oxide production inhibitory activity of essential oil from *Geophila repens* (L.) I.M. Johns, Molecules 22 (2017) 1–13.

[19] A.K. Sahoo, U.C. Dash, S. Kanhar, A.K. Mahapatra, *In vitro* biological assessment of *Homalium zeylanicum* and isolation of lucidenic acid A triterpenoid, Toxicol. Rep. 4 (2017) 274–281.

[20] H. Sies, W. Stahl, Vitamins E and C, β-carotene, and other carotenoids as antioxidants, Am. J. Clin. Nutr. 62 (1995) 1315–1321.

[21] W. Stahl, H. Sies, Antioxidant activity of carotenoids, Mol. Aspects Med. 24 (2003) 345–351.

[22] E. González-Burgos, M.P. Gomez-Serranillos, Terpene compounds in nature: a review of their potential antioxidant activity, Curr. Med. Chem. 19 (2012) 5319–5341.

[23] L. Gu, X. Weng, Antioxidant activity and components of *Salvia plebeia* R.Br.–a Chinese herb, Food Chem. 73 (2001) 299–305.

[24] M.J.R. Howes, N.S. Perry, P.J. Houghton, Plants with traditional uses and activities, relevant to the management of Alzheimer's disease and other cognitive disorders, Phytother. Res. 17 (2003) 1–18.

[25] N. Jamila, K.K. Yeong, V. Murugaiyah, A. Atlas, I. Khan, N. Khan, S.N. Khan, M. Khairuddean, H. Osman, Molecular docking studies and *in vitro* cholinesterase enzyme inhibitory activities of chemical constituents of *Garcinia hombroniana*, Nat. Prod. Res. 29 (2015) 86–90.